Effects of bending portions of the air column on the acoustical resonances of a wind instrument

Simon Félix, Jean-Pierre Dalmont

Effects of bending portions of the air column on the acoustical properties of a wind instrument

Simon Félix[a)] and Jean-Pierre Dalmont

LAUM,

CNRS,

Université du Maine,

avenue Olivier Messiaen,

72085 Le Mans,

France.

C. J. Nederveen

Acacialaan 20,

2641 AC Pijnacker,

Netherlands

(Dated: November 18, 2011)

Abstract

The need to keep long wind musical instruments compact imposes the bending of portions of the air column. Although manufacturers and players mention its effects as being significant, the curvature is generally not included in physical models and only a few studies, in only simplified cases, attempted to evaluate its influence. The aim of the study is to quantify the influence of the curvature both theoretically and experimentally. A multimodal formulation of the wave propagation in bent ducts is used to calculate the resonances frequencies and input impedance of a duct segment with a bent portion. From these quantities an effective length is defined. It displays a dependence to frequency such that, compared to an equivalent straight tube, the shift in resonance frequencies in a tube with bent sections is not always positive, as generally stated. The curvature not always increases the resonances frequencies, but may even decrease them, resulting in a complex inharmonicity. An experimental evidence of the effect of the curvature is also shown, with a good agreement with theoretical predictions.

PACS numbers: 43.75.Ef, 43.75.Fg 43.20.Mv,

I. INTRODUCTION

Long wind musical instruments are often made with bends to keep them compact. Although it is generally stated, following Rayleigh's argument, that "*straightness is not a matter of importance*"[1], bending portions of the air column may in somes cases affect the tuning in a musically significant way. Several authors, then, attempted to quantify the effect of the curvature on the tuning. Nederveen[2] (completed in[3]), and later Keefe and Benade[4], showed that in a bent duct, in the long wavelength limit, the inertance is lowered relative to its value in a straight duct having the same cross-section:

$$\mathcal{L}_{\text{bend}} = \alpha \mathcal{L}_{\text{straight}}, \tag{1}$$

where

$$\alpha = \frac{\frac{1}{2}\kappa^2}{1 - \sqrt{1-\kappa^2}} < 1, \tag{2}$$

with $\kappa = a/R_0$ the axis curvature[5] (Fig. 1). The curvature induces an increase in resonance frequencies. In other words, the length correction due to the curvature in a duct is negative: $\Delta L < 0$. Experimental studies reported in the litterature[3,4,6] confirm this qualitative result at low frequency. Following, methods for compensating bends in air columns when designing wind instruments have been proposed, as, for example, a reduction of the bore diameter at bends[2,3,6,7].

However, reducing the bore diameter at bends to compensate for the tuning change supposes that this change is weakly frequency-dependent, or, at least, that the frequency shift, or the length correction, remains the same sign over the musically useful frequency range.

It is shown in the present paper that the frequency shift, or the length correction, in a bend, may vary significantly over frequency and that its sign changes. The curvature not always increases the resonance frequencies, but may even decrease them, resulting in a

[a)]Electronic address: simon.felix@univ-lemans.fr

complex inharmonicity. Two ways of characterising the effect of the curvature are described in the following: the computation of the resonances frequencies in a duct with a bend (section 2), and the computation of its input impedance (section 3). The results for both methods are shown and discussed (section 4), and an experimental characterization is then given (Section 5).

II. RESONANCES IN A DUCT WITH A BEND

For the sake of clarity and to clearly point out the effect of bending, the air column is supposed to be composed of straight and bent segments with a constant, circular, cross-section. As any such bend can be represented through a succession of straight and bent segments, we will consider in the following the very simple wind instrument drawn in Fig. 1 to show the influence of the curvature.

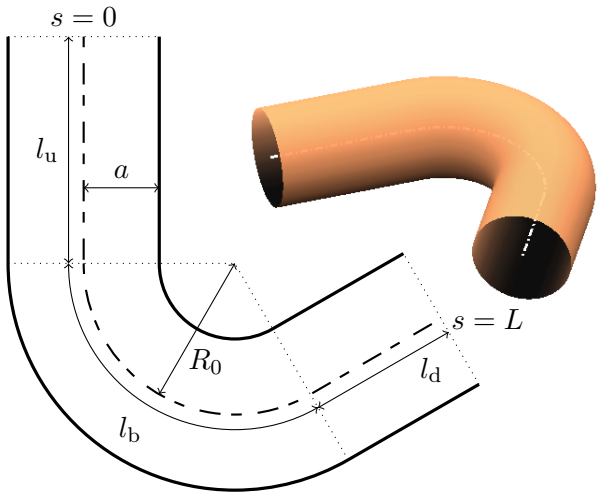

FIG. 1. Duct with a bent portion. s is the abscissa along the waveguide axis, measured from the input of the duct (top), and $L = l_\mathrm{u} + l_\mathrm{b} + l_\mathrm{d}$ is the total length of the duct axis.

We restrict on frequencies below the first cutoff in the straight segment, that is, wavenumbers below $k_\mathrm{c} = \gamma_{10}/a$, with a the duct radius and $\gamma_{10} \simeq 1.8412$ the first positive zero of the first derivative of the Bessel function of the first kind J_1.

A. Scattering matrix of the duct

At each extremity of the duct, the wave field can be expressed as a sum over the local transverse modes, that is, the classical solutions of the transverse eigenproblem $\Delta_\perp \phi_n = -\alpha_n^2 \phi_n$ in the circular cross-section, with the homogeneous Neumann boundary condition at the walls[8,9]: $p = \sum_{n\geq 0} P_n \phi_n = {}^t\vec{\phi}\vec{P}$. The components of the wave field in the basis $\{\phi_n\}$ can be splitted into ingoing waves $\vec{A}$ and outgoing waves $\vec{B}$, both at the input end of the duct ($s = 0$, s the abscissa along the waveguide axis) and at the output end ($s = L$, cf. Fig. 1).

The scattering matrix of the duct relates outgoing waves to incoming waves:

$$\begin{pmatrix} \vec{B}^{(0)} \\ \vec{B}^{(L)} \end{pmatrix} = S \begin{pmatrix} \vec{A}^{(0)} \\ \vec{A}^{(L)} \end{pmatrix}. \tag{3}$$

For such a simple geometry of duct, it can be algebraically calculated.[8]

Given the boundary conditions at each end of the duct and its scattering matrix, the resonances can be found as the frequency solutions $k_i^{(\kappa)}$ of a dispersion relation. For example, if one imposes at the output end a Dirichlet condition $p = 0$, as the simplest, non radiating, open end condition, and a Neumann condition $\partial_s p = 0$ at the input end, the dispersion relation is

$$\det \left[S - \begin{pmatrix} I & 0 \\ 0 & -I \end{pmatrix} \right] = 0, \tag{4}$$

I the identity matrix.

An example of solution of the above equation (4) is shown in Tab. I, giving the first resonance frequencies in a duct as shown in Fig. 1, and their relative difference with the resonance frequencies in a straight duct having the same dimension L/a, that is, under the first cut-off,

$$k_i^{(0)} = \left(i - \frac{1}{2} \right) \frac{\pi}{L}, \quad i = 1, 2, 3 \ldots \tag{5}$$

(note that the solutions of Eq. (4) with a zero curvature, computed with 12 modes ϕ_n, differ from the theoretical results above by less than 10^{-12} %, thus mainly limited by the machine precision). The dependence to frequency of the shift in resonance frequencies can be seen

here, from positive to negative shifts. Although it has not been explicitely noted, this effect of the curvature was already apparent in results shown in Ref.[8] on resonances in annular cavities (see Tab. 1 and Fig. 5 of cited Ref.).

In the following, we consider the effect of curvature in term of a correction, frequency dependent, to the apparent length of the duct. This length correction is simply related to the solutions of Eq. (4) by

$$\Delta L_i = \left(\frac{k_i^{(0)}}{k_i^{(\kappa)}} - 1 \right) L. \tag{6}$$

B. Finite differences

Resonance frequencies of the pipe combinations were independently computed numerically using the finite difference method (FDM). Studied were the situations with open end (Fig. 3) and closed end (Fig. 11). In the first case the pressure was set to zero at the pipe end, and in the second case the velocity was zero. In the latter case the following discretization expression for the second derivative of the pressure in the axial direction is used

$$\frac{\partial^2 p}{\partial s^2} = \frac{2p_{-1} - 2p_0}{h^2} + \mathcal{O}(h). \tag{7}$$

More elaborate expressions are possible[10]; they were tried, but were found to give no improvement. The effect of the bend was found by comparing two pipe combinations of the same length, one without and one with a bend. The frequency was varied until either the input pressure or the input velocity was zero, corresponding to zero or infinite impedance. Although the frequency of a straight pipe can also be analytically determined, the FDM results were preferred, since the limited number of grid points resulted in small systematic errors; they were assumed to be the same for straight and curved pipes. The velocity v_0, or rather a quantity q_0 proportional to the velocity, at an in-between-point was calculated from the pressures: $q_{0.5} = p_1 \breve{} p_0$, likewise $q_{1.5} = p_2 \breve{} p_1$. The velocity at the input was obtained by extrapolation from these values. In the FDM procedure the circular space of the cross-section is filled with rectangles, causing irregular fluctuations in the results. By plotting

against the reciprocal of the number of points and levelling fluctuations, the results for an "infinite" number of points was obtained by extrapolation. The frequency corrections were recalculated in length corrections with Eq. (6) and referred to the tube radius. The accuracy of the end result is estimated to be ± 0.02.

III. INPUT IMPEDANCE OF A DUCT WITH A BENDING PORTION

Classically, the resonator that composes a wind instrument is characterized by calculating or measuring its input impedance $z_{\text{in}} = \bar{p}^{(\text{in})}/A\bar{v}_s^{(\text{in})}$ as function of the frequency, where $\bar{p}^{(\text{in})}$ and $A\bar{v}_s^{(\text{in})}$ are, respectively, the mean pressure and volume velocity at the input end of the duct, with $A = \pi a^2$ the cross-section area. The impedance proves valuable to study the linear acoustic properties of the instrument, since, in particular, its peaks are strongly linked to the playing frequencies of the instrument.

A. Computation of the input impedance

For a cylindrical duct, considering only the propagation of plane waves ($k < k_{\text{c}}$), the input impedance is given by

$$z_{\text{in}} = z_{\text{c}} \tanh\left(-\text{j}kL + \text{atanh}\left[\frac{z_{\text{r}}}{z_{\text{c}}}\right]\right), \tag{8}$$

with z_{r} the value of the impedance at the output, $z_{\text{c}} = \rho_0 c_0/A$ the characteristic impedance, ρ_0 the density of air, and c_0 the sound velocity.

In a duct with bent portions, even under the cutoff frequency k_{c}, the variations of the pressure or velocity over the cross-section are not negligible[8,11]. Higher order modes, even though they are evanescent, must be taken into account. To do this, the volume velocity is expressed as a sum over the transverse modes, as was done previously for the pressure: $Av_s = \sum_{n\geq 0} U_n\phi_n = {}^t\vec{\phi}\vec{U}$. Then, one defines an impedance matrix, fulfilling $\vec{P} = Z\vec{U}$. As

the scattering matrix (see above), the impedance matrix can be algebraically calculated in a simple geometry such as the one considered here.[12]

Once the output condition is expressed as a matrix Z_r, the input impedance matrix $Z^{(\mathrm{in})}$ of the duct is calculated. As, by definition, $P_0 = \bar{p}$ and $U_0 = A\bar{v}_s$, we can write

$$\bar{p}^{(\mathrm{in})} = Z_{00}^{(\mathrm{in})} A\bar{v}_s^{(\mathrm{in})} + \sum_{n>0} Z_{0n}^{(\mathrm{in})} U_n. \tag{9}$$

Below the first cut-off and far from discontinuities, sources, or other regions where a mode coupling may occur, $U_{n>0} \to 0$. Thus, providing that l_u is large enough,

$$z_\mathrm{in}^{(\kappa)} = \frac{\bar{p}^{(\mathrm{in})}}{A\bar{v}_s^{(\mathrm{in})}} \simeq Z_{00}^{(\mathrm{in})}. \tag{10}$$

In the straight duct, the relative error between $Z_{00}^{(\mathrm{in})}$, when 12 modes are taken into account, and z_in as given by Eq. (8), is in the order of magnitude of $10^{-15} - 10^{-13}$, certainly depending on the computer precision.

Fig. 2 shows an example of computation of the impedance $z_\mathrm{in}(k)$ at the input of the duct studied above (see Tab. I). Again, the comparison with the result for a straight duct shows a frequency dependent shift, the sign of which changes near $k/k_\mathrm{c} = 0.5$.

B. Length correction

From the input impedance, using Eq. (8), an effective length of the duct can be defined:

$$L_\mathrm{eff.} = \mathrm{Re}\left[-\frac{1}{\mathrm{j}k}\left(\mathrm{atanh}\left[\frac{z_\mathrm{in}^{(\kappa)}}{z_\mathrm{c}}\right] - \mathrm{atanh}\left[\frac{z_\mathrm{r}}{z_\mathrm{c}}\right]\right)\right], \tag{11}$$

leading to the length correction

$$\Delta L(k) = L_\mathrm{eff.} - L. \tag{12}$$

IV. RESULTS

The length correction corresponding to the impedance in Fig. 2 is given in Fig. 3, together with the resonance frequencies obtained with both Eq. (4) and the FDM. This plot clearly

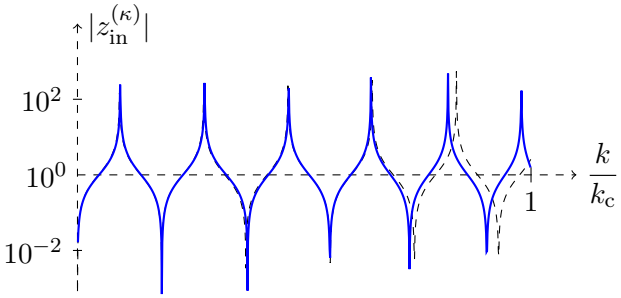

(a) Modulus

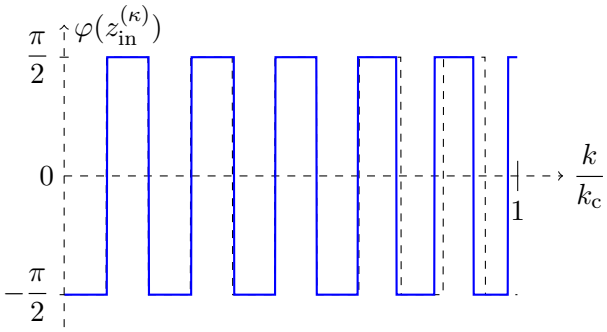

(b) Phase

FIG. 2. Input impedance of the duct shown in Fig. 1, with $l_{\mathrm{u}}/a = 3$, $l_{\mathrm{b}}/a = 4\pi/3$, $l_{\mathrm{d}}/a = 2$, and a Dirichlet boundary condition $p = 0$ at the output end ($s = L$). The results, given for a curvature $\kappa = 0.5$ of the bend axis and computed with 12 modes taken into account (solid curve), are compared with the "reference" input impedance of a straight duct ($\kappa = 0$, dashed) with the same axis length L/a.

points out the strong dependence with frequency of the mistuning induced by the bending. As reported in earlier studies[2–4,6,7], the length correction at low frequencies is negative. When increasing the frequency, it becomes smaller in absolute value (some oscillations can be observed, they are discussed in the following), to reach zero at a frequency close to $k_{\mathrm{c}}/2$. Then its sign changes and it increases, until it reaches, near the cutoff, a value that is generally comparable to its value at zero frequency, with opposite sign. Furthermore, in this example (the drawnings in Fig. 1 show the dimensions of the duct), the length correction is far from negligible, varying in absolute value from 0 to a quarter of the radius a.

It may be noted that the solid curve is not drawn until the cutoff frequency. The limit

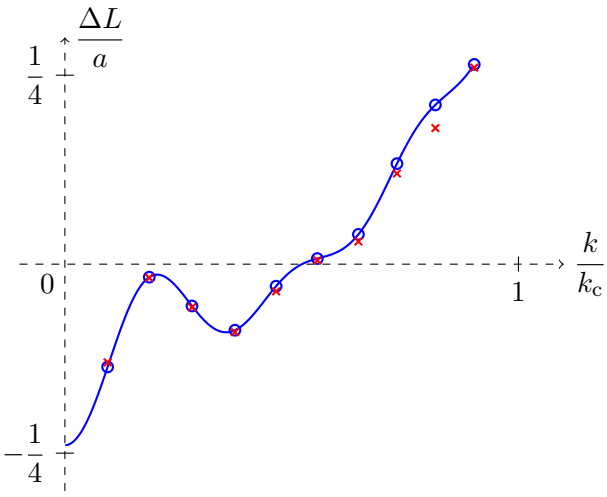

FIG. 3. Length correction, in tube radius unit, for the duct shown in Fig. 1, with $\kappa = 0.5$, $l_u/a = 3$, $l_b/a = 4\pi/3$, $l_d/a = 2$, and a Dirichlet boundary condition $p = 0$ at the output end ($s = L$). Solid line: length correction as defined by Eqs. (11-12) with the input impedance shown in Fig. 2, 'o': solutions of the dispersion relation (4) with a Neumann or a Dirichlet condition at the input end, '×': finite differences method.

of validity of the definition (11-12) of the length correction is, practically, below the first cutoff frequency, as soon as the higher order modes, although still evanescent, can no longer be considered as a small perturbation.

When varying the curvature of the bent portion, while keeping constant the lengthes l_u, l_b and l_d, the evolution with frequency of length correction is roughly the same, with mainly the overall amplitude of the curve changing: the larger the curvature, the larger the length correction, or, in other words, the stronger the mistuning (Fig. 4). At a given frequency, the length correction increases roughly as the square of the curvature κ (Fig. 5).

Besides, two remarks can be made from the results in Fig. 4:

1. whatever the curvature, the length correction becomes very small around $k/k_c = 0.2$,

2. the results reveal a low dependence on the curvature of the frequency at which the

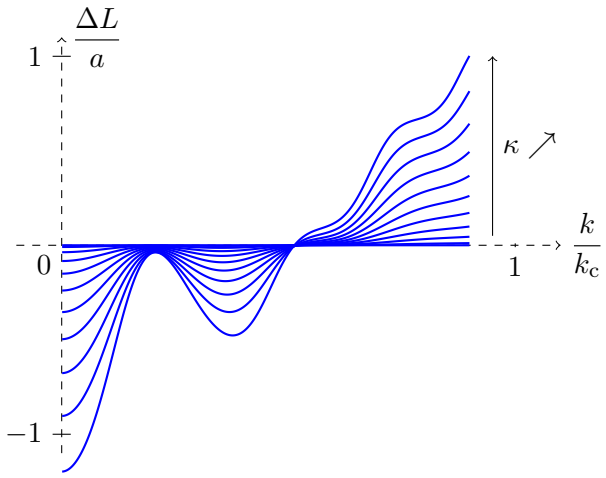

FIG. 4. Influence of the curvature on the length correction, as defined by Eqs. (11-12). The value of κ is increased from 0 to 1, in steps of 0.1 between curves.

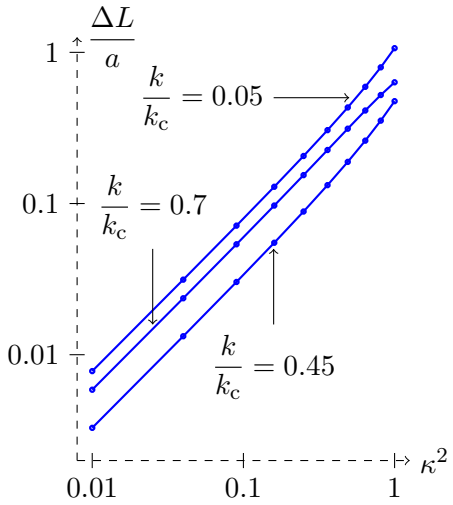

FIG. 5. Influence of the curvature on the length correction, as defined by Eqs. (11-12): ΔL increases as, roughly, the square of κ, at a given frequency.

change in sign occurs: it remains near $k_c/2$.

1. Minima of the length correction

Previous studies described the effect of bending a duct as a perturbation of the inertance,[2–4] lowered relative to its value in a straight duct (Eqs. 1-2). Following this low

frequency description, one may expect this effect to vanish, or at least be lowered, when the position of the bend in a duct coincides with a node of the longitudinal velocity field. Indeed, if one supposes that the velocity node is located at the center of the bend in the example of Fig. 3, it follows that $\lambda/4 = l_\mathrm{b}/2 + l_\mathrm{d}$, λ the wavelength. Thus,

$$\frac{k}{k_\mathrm{c}} = \frac{\pi a}{(l_\mathrm{b} + 2l_\mathrm{d})\gamma_{10}} \simeq 0.2084. \tag{13}$$

If one varies the distance l_d from the output to the bend while keeping constant the curvature κ, the axis length of the bend l_b, and the overall length of the duct L, one observes a displacement of this local minimum of $|\Delta L|$ according to the above equation. The length correction does not exactly reach zero, because at this frequency, the wavelength ($\lambda/a \simeq 16.4$) is not large compared with the length of the bend ($l_\mathrm{b}/a \simeq 4.2$). Thus, the velocity field is not zero or negligible in the whole bend.

Besides, one can deduce that the length correction for a long duct with a bent portion will exhibit a large number of local minima (Fig. 6). In this case, the first minima appear at long waveglengthes, compared with the bend size, therefore the length correction $|\Delta L|$ is very close to zero at these frequencies.

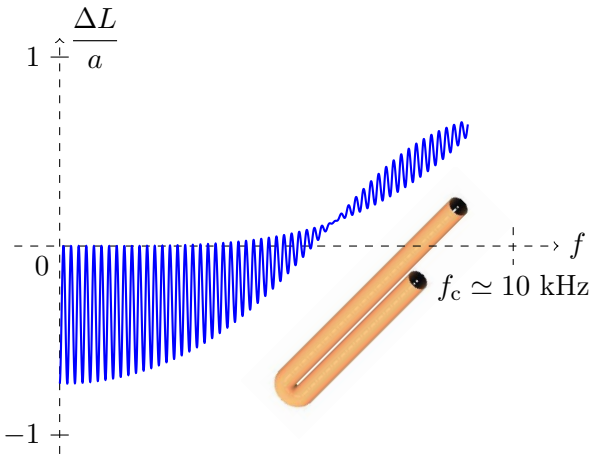

FIG. 6. Length correction, in tube radius unit, for a "bassoon-like" duct, with $a = 0.01$ m, $\kappa = 0.91$, $l_\mathrm{u} = 1.3$ m, $l_\mathrm{b} = \pi a/\kappa$, $l_\mathrm{d} = 1$ m, and a Dirichlet boundary condition $p = 0$ at the output end ($s = L$).

2. *Frequency of the sign change*

For frequencies below, and not too close to, the first cutoff k_c, the properties of the bent segment, notably the way the length correction varies with frequency, are mainly related to the characteristics of the first bend mode. In contrary to the *local* transverse modes ϕ_n that are used in the multimodal method (see Sec. II and Ref.[8]), the bend modes, solutions of the transverse eigenproblem in a toroidal bend, can not be calculated analytically. However, if one considers the infinite matricial equation governing $\vec{P}$ in a bend:

$$\partial_{ss}^2 \vec{P} + M\vec{P} = \vec{O}, \tag{14}$$

where M is a matrix depending on the basis $\{\phi_n\}$ and the curvature κ, the bend modes appears as being the basis that diagonalizes this matrix.[11,13] It is thus possible to approximate these solutions, and in particular the first bend mode $\breve{\phi}_0$ and its associated propagation constant $\breve{k}_0$, by computing the eigenmodes of the truncated matrix M. The propagation constant $\breve{k}_0$ is an increasing function of k that is lower than k at low frequencies and higher than k near the cut-off k_c (Fig. 7). Note that a similar observation was made by Cummings[14] in bends with rectangular cross-section, and borne out by El-Raheb[15]. Therefore, if one assumes that the effect of the curvature at low frequencies is, roughly, to replace the plane wave propagating with a wave number k by a quasi-plane wave propagating with the wave number $\breve{k}_0$, this explains qualitatively the variations of ΔL and the sign change.

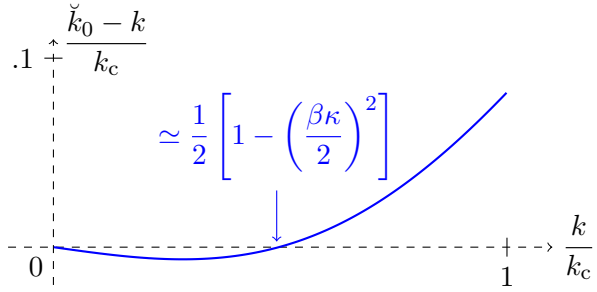

FIG. 7. Evolution with frequency of the propagation constant $\breve{k}_0$ of the first bend mode in a bend with curvature $\kappa = 0.5$, computed with 12 modes taken into account.

If one takes into account only 2 modes in the multimodal formulation - the plane wave mode ϕ_0 and the first evanescent mode ϕ_1, a simple approximation for $\breve{k}_0$ can be analytically calculated:

$$\breve{k}_0 = \Bigg[k^2(1+\beta^2\kappa^2) + \dots \\ \frac{1}{2}\left(\sqrt{k_\mathrm{c}^4 - 8\beta^2\kappa^2k^2(k_\mathrm{c}^2-2k^2)} - k_\mathrm{c}^2\right)\Bigg]^{1/2} \tag{15}$$

where

$$\beta = \frac{1}{\gamma_{10}^2\sqrt{\frac{1}{2}\left(1-\frac{1}{\gamma_{10}^2}\right)}} \lesssim \frac{1}{2}. \tag{16}$$

It differs from the "converged" value, computed with 12 modes (Fig. 7), by less than 0.3%. The frequency at which $\breve{k}_0(k) = k$ is

$$k_\mathrm{s} = \frac{k_\mathrm{c}}{2}\left[1 - \left(\frac{\beta\kappa}{2}\right)^2\right]. \tag{17}$$

It is weakly dependent of the curvature: the relative shift from $k_\mathrm{c}/2$ varies between 0 and $\sim 6\%$.

Of course, from this result, the rigorous calculation that would lead to the properties of the length correction itself is not straightforward, but this gives basic elements to better understand how a bend modify the propagation and resonances in a duct.

Another remark can be made from the results on $\breve{k}_0$: the inertance correction (2) was first deduced by Nederveen[2] from a simplified formulation of the conservation equations in the long wavelength limit:

$$\frac{\partial \bar{v}_s}{\partial s} = \frac{\mathrm{j}k}{\rho_0 c_0}\bar{p}, \tag{18}$$

$$\frac{\partial \bar{p}}{\partial s} = \mathrm{j}k\alpha\rho_0 c_0 \bar{v}_s. \tag{19}$$

If, in a rough approximation, a low frequency wave in a bend is assumed to propagate with a wavenumber $\breve{k}_0$, then the coefficient α should be related to the zero frequency limit of

$(\breve{k}_0/k)^2$. Indeed, the relative difference between α and this limit remains under 5% until $\kappa \simeq 0.96$ (Fig. 8).

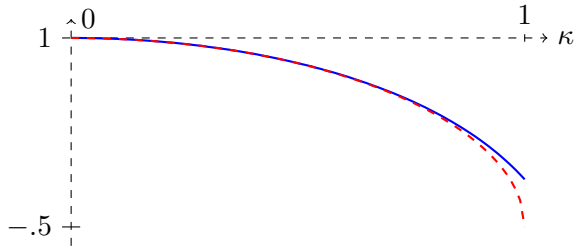

FIG. 8. Solid curve: zero frequency limit of $(\breve{k}_0/k)^2$, as approximated by its value at $k/k_c \simeq 5.10^{-6}$, computed with 12 modes taken into account, as a function of the curvature. Dashed curve: inertance correction α (Eq. 2).

V. EXPERIMENTAL EVIDENCE OF THE FREQUENCY SHIFT DUE TO THE CURVATURE

In order to obtain an experimental characterization of the length correction of a bend, a duct with a circular cross-section and a toroidal bent portion has been designed (Fig. 9) and its input impedance is measured using a set-up developed joinly by LAUM and CTTM.[16,17] It consists in placing at the input of the measured instrument a piezo-electric source with a back closed cavity. While a first microphone measures the pressure at the input of the instrument, a second microphone measures the pressure in the back cavity. Assuming the latter to be proportional to the volume velocity of the source, the input impedance of the measured object is then simply calculated from the transfer function between the two microphones. The reader may refer to Ref.[18] for details on this set-up.

The frequency range of interest (from zero to the first cutoff $f_c \simeq 5.76$ kHz), is decomposed in four overlapping intervals, in order to maximize the SNR without saturation of the measured signal. For each interval, a one second long logarithmic chirp is used as input signal, leading to a frequency resolution of 1 Hz. The temperature in the tube is estimated by a prior measurement of the input impedance of a closed cylindrical tube of known di-

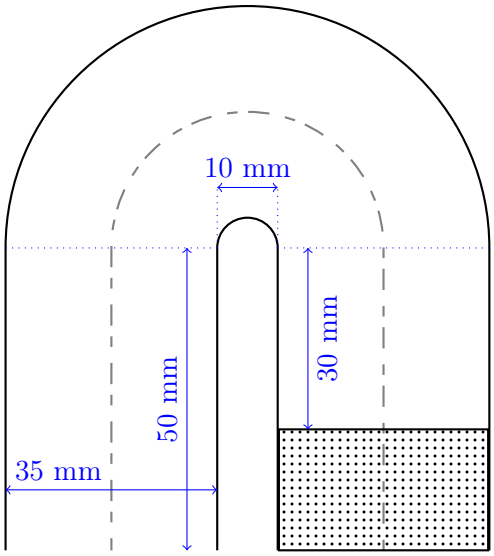

FIG. 9. Dimensions of the duct designed for the experiments. The axis curvature of the bend is $\kappa = 7/9$ and the duct is closed at the output.

mensions. For each tube, the acquisition is repeated 5 times and averaged. The calibration of the impedance sensor is described in the paper by Macaluso and Dalmont.[18] The residual error is evaluated by calculating the difference between the measured input impedance of the straight tube with the theoretical value. Then the difference is used (except at its "singularities", that is, at the resonances of the straight tube) as a correction to the measured input impedance of the curved tube.

The measured input impedance is shown in Fig. 10. It is compared with the theoretical input impedance, computed as described earlier in the paper. To take into account the viscothermal losses at the walls in the multimodal formulation, the purely real or purely imaginary propagation constants of the modes ϕ_n are replaced by complex propagation factors.[19,20] Note, however, that this way of introducing the losses is not fully rigorous, as it assumes that the wall on which the boundary layer lies is locally plane. Therefore the effet of the curvature of the boundary layer is not taken into account. Further investigations will be made on this particular aspect.

Fig. 11 shows the comparison of the measured length correction (from the experimental

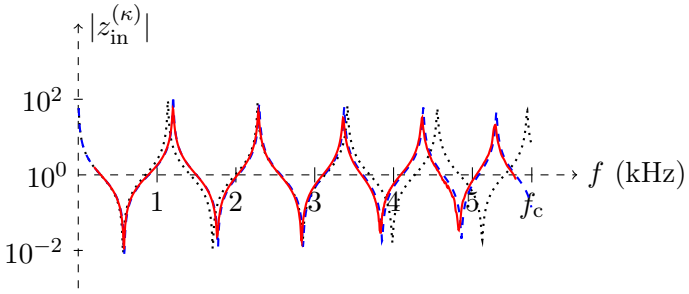

(a) Modulus

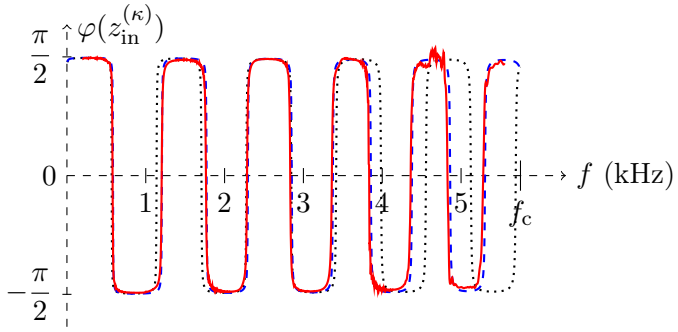

(b) Phase

FIG. 10. Solid curve: measured input impedance of the duct shown in Fig. 9, with $a = 0.0175$ m, $\kappa = 7/9$, $l_{\text{u}} = 0.05$ m, $l_{\text{b}} = \pi a/\kappa$ m, $l_{\text{d}} = 0.03$ m, closed at its output end. Dashed curve: Theoretical input impedance. Dotted curve: Theoretical input impedance of a straight duct having the same radius and length.

input impedance of Fig. 10) with the theoretical and numerical results from the multimodal and finite difference methods. The agreement is good on the whole frequency range. The shift of about 0.05 between the two curves can be explained by a possible temperature difference between the two measured tubes and the uncertainty in the temperature evaluation from the input impedance of the straight tube.

VI. CONCLUSION

The effects of bending a portion of a duct have been investigated theoretically and experimentally. Results show that the frequency shift induced by the curvature is not always

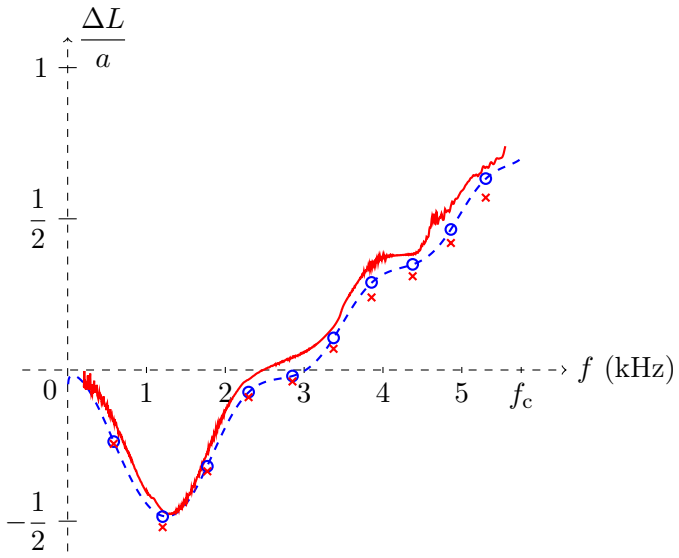

FIG. 11. Length correction, in tube radius unit, for the duct shown in Fig. 9, with $a = 0.0175$ m, $\kappa = 7/9$, $l_u = 0.05$ m, $l_b = \pi a/\kappa$ m, $l_d = 0.03$ m, closed at its output end. Solid curve: experimental result. Dashed curve: theoretical result, as defined by Eqs. (11-12) with the theoretical input impedance shown in Fig. 10. 'o': solutions of the dispersion relation (4) with a Neumann or a Dirichlet condition at the input end, '×': finite differences method.

small and, moreover, is strongly frequency dependent. It notably exhibit a sign change, so that the first resonance frequencies in a bent tube are shifted towards higher values, while they are shifted towards lower values near the cutoff. It has been shown that the magnitude of the frequency shift varies, roughly, as the square of the curvature, and that the frequency of the sign change is weakly dependent on the curvature.

Two characteristics of the wave propagation within the air column of an instrument shall now be investigated, for which one may expect significant effects to be observed. First, the losses in the fluid or at the walls: in the present paper, only lossless or weakly lossy cases have been considered. Earlier studies have shown, however, the significant infuence of the curvature on the wave propagation in lined bend, notably the effect of localized wall losses[12]. Second, the non linear propagation, since high pressure levels can be measured in the air column of musical instruments.

Acknowledgments

The authors wish to thank Joël Gilbert for fruitfull discussions.

References

[1] J. W. S. Rayleigh, *Theory of Sound*, volume 2, section 263 (McMillan and Company, London) (1878).

[2] C. J. Nederveen, *Acoustical aspects of woodwind instruments*, chapter 37 (Knuf, Amsterdam) (1969).

[3] C. J. Nederveen, "Influence of a toroidal bend on wind instrument tuning", J. Acoust. Soc. Am. **104**, 1616–1626 (1998).

[4] D. H. Keefe and A. H. Benade, "Wave propagation in strongly curved ducts", J. Acoust. Soc. Am. **74**, 320–332 (1983).

[5] Expressions of the length correction by Nederveen[2] and Keefe and Benade[4] are analytically identical, as mentionned by Nederveen[3].

[6] G. S. Brindley, "Speed of sound in bent tubes and the design of wind instruments", Nature **246**, 479–480 (1973).

[7] J. W. Coltman, "Compensating for miter bends in cylindrical tubing", J. Acoust. Soc. Am. **121**, 2497–2498 (2007).

[8] S. Félix and V. Pagneux, "Multimodal analysis of acoustic propagation in three-dimensional bends", Wave Motion **36**, 157–168 (2002).

[9] Practically, modes are sorted by increasing order of their cutoff frequency, from $n = 0$ (plane wave) to infinity, and the series are truncated to a finite number of modes for numerical computations.

[10] D. Zwillinger, *Handbook of differential equations*, chapter 4 (Academic Press, New York) (1992).

[11] S. Félix and V. Pagneux, "Sound propagation in rigid bends: A multimodal approach", J. Acoust. Soc. Am. **110**, 1329–1337 (2001).

[12] S. Félix and V. Pagneux, "Sound attenuation in lined bends", J. Acoust. Soc. Am. **116**, 1921–1931 (2004).

[13] C. K. W. Tam, "A study of sound transmission in curved duct bends by the Galerkin method", J. Sound Vib. **45**, 91–104 (1976).

[14] A. Cummings, "Sound transmission in curved duct bends", J. Sound Vib. **35**, 451–477 (1974).

[15] M. El-Raheb, "Acoustic propagation in rigid three-dimensional waveguides", J. Acoust. Soc. Am. **67**, 1924–1930 (1980).

[16] LAUM: Laboratoire d'Acoustique de l'Université du Maine, CNRS, Université du Maine, avenue Olivier Messiaen, 72085 Le Mans, France. CTTM: Centre de Transfert de Technologies du Mans, 20 rue Thalès de Millet, 72000 Le Mans, France.

[17] J.-P. Dalmont and J.-C. Le Roux, "A new impedance sensor for wind instruments (A)", J. Acoust. Soc. Am. **123**, 3014 (2008).

[18] C. A. Macaluso and J.-P. Dalmont, "Trumpet with near-perfect harmonicity: Design and acoustic results", J. Acoust. Soc. Am. **129**, 404–414 (2011).

[19] A.-M. Bruneau, M. Bruneau, P. Herzog, and J. Kergomard, "Boundary layer attenuation of higher order modes in waveguides", J. Sound Vib. **119**, 15–27 (1987).

[20] N. Amir, V. Pagneux, and J. Kergomard, "A study of wave propagation in varying cross-section waveguides by modal decomposition - part II: Results", J. Acoust. Soc. Am. **101**, 2504–2517 (1997).

$\kappa = 0$	$\kappa = 0.5$	%Diff
0.092(8)	0.094(2)	+ 1.5%
0.278(5)	0.280(2)	+ 0.6%
0.464(2)	0.465(8)	+ 0.3%
0.649(9)	0.647(3)	− 0.4%
0.835(6)	0.817(2)	− 2.2%

TABLE I. Resonance frequencies $k_i^{(\kappa)}/k_\mathrm{c}$, k_c the first cutoff in the straight segments, in the duct shown in Fig. 1, with $l_\mathrm{u}/a = 3$, $l_\mathrm{b}/a = 4\pi/3$, $l_\mathrm{d}/a = 2$, an homogeneous Neumann boundary condition $\partial_s p = 0$ at the input end ($s = 0$), and an homogeneous Dirichlet boundary condition $p = 0$ at the output end ($s = L$). The results, given for a curvature $\kappa = 0.5$ of the bend axis and computed with 12 modes ϕ_n taken into account, are compared with "reference" resonance frequencies in a straight duct ($\kappa = 0$) with the same axis length L/a.

List of Figures